

## Photophysical and photochemical properties of a novel thiol terminated low symmetry zinc phthalocyanine complex and its gold nanoparticles conjugate

Cite this: *Dalton Trans.*, 2013, **42**, 4922

Thandekile P. Mthethwa,<sup>a</sup> Sinem Tuncel,<sup>b</sup> Mahmut Durmuş<sup>b</sup> and Tebello Nyokong<sup>\*a</sup>

A novel thiol functionalized zinc phthalocyanine complex (ZnPcSH) is reported in this work. This complex was conjugated to gold nanoparticles. The photophysical and photochemical properties of the complex and the conjugate were investigated. Upon conjugation a blue shift was observed from the UV-Vis spectra. The conjugate showed a decrease in the fluorescence quantum yield and lifetime. An increase in the triplet quantum yield and lifetime was observed for ZnPcSH following conjugation to gold nanoparticles. Both ZnPcSH and its conjugate with gold nanoparticles showed high singlet oxygen quantum yields with the conjugate being higher than the Pc alone.

Received 12th November 2012,  
Accepted 22nd January 2013

DOI: 10.1039/c3dt32698e

[www.rsc.org/dalton](http://www.rsc.org/dalton)

### Introduction

Metallophthalocyanines (MPcs) have attracted a lot of interest lately as photosensitizers for photodynamic therapy (PDT). PDT involves the use of light to excite the photosensitizer to its triplet state, this allows interaction with molecular oxygen and production of the cytotoxic singlet oxygen that destroys the tumor cells.<sup>1</sup> MPcs have been a subject of interest because of their applications in other areas such as sensors,<sup>2</sup> photocatalysis<sup>3</sup> and optical limiting.<sup>4</sup> The introduction of substituents onto the peripheral and non-peripheral positions of the ring improves the solubility of the Pcs and allows for further conjugation. The metallophthalocyanine complexes containing alkylthio or arylthio ring substituents have been the most explored.<sup>5–8</sup> These phthalocyanine complexes show a red shifted Q band which makes them good candidates for PDT. Functionalized phthalocyanine complexes containing terminal SH groups have been less studied due to the difficulty of the synthesis.<sup>9–12</sup> These complexes readily form S–S bonds in air.

Conjugates of phthalocyanines and Au nanoparticles (AuNPs) have been reported for drug delivery applications.<sup>9,10</sup> The conjugates reported in the literature used phthalocyanines which are substituted at the periphery with thiol groups. We have also reported on the conjugation of AuNPs using a Pc containing one SH or tetrasubstituted with SH groups.<sup>11</sup> The reported complexes contained an alkyl linker to the SH group.

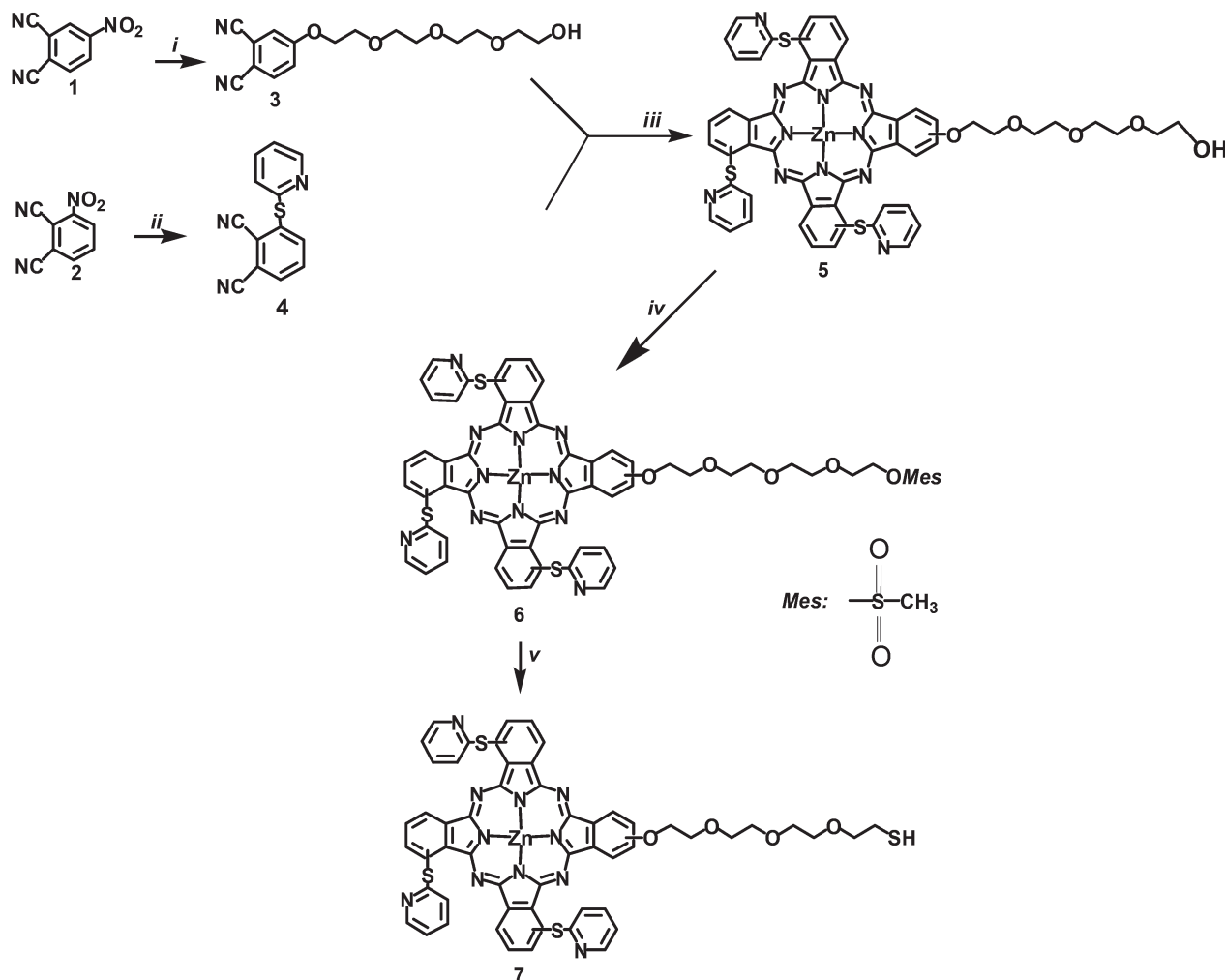
This work reports on the use of an ethoxy group as a linker to the SH group.

The ethoxy groups were chosen because ethoxy substituted Pc compounds have shown a very high singlet oxygen quantum yield.<sup>12</sup> The other three positions in the tetrasubstituted ring contain mercapto pyridyl groups for enhanced solubility and red shifting on the Q band, both are requirements for use of Pcs in PDT. The mercapto pyridyl groups could also provide another point of attachment of the AuNPs. The complex reported in this work is: 1,8(11),15(18)-tri-(2-mercapto-pyridine)-23(24)-4-(2-[2-(2-mercaptoethoxy)-ethoxy]ethoxy)-ethoxy phthalocyaninato zinc(II) (7, abbreviated as ZnPcSH, Scheme 1).

The use of gold nanoparticles in delivery applications is based on the possible use of the conjugates in enhanced permeability and retention (EPR) effect in which the conjugates can be taken up by tumor cells and be retained.<sup>13</sup> Gold nanoparticles have been studied extensively for biomedical applications owing to their interesting plasmonic properties and non-toxic nature. Their chemical and physical properties have made them very useful in diagnostics,<sup>14</sup> biosensing<sup>15</sup> and drug delivery.<sup>16</sup> The position of the plasmonic peak is greatly dependent on the size and morphology of AuNPs; therefore studies have been directed to the synthesis of monodispersed gold nanoparticles with controlled sizes.<sup>17–20</sup> The fabrication of gold nanoparticles has been extended to the modification of their surfaces with different ligands to allow for bioconjugation.<sup>21–24</sup> In this study, the photophysical properties of the conjugates of ZnPcSH with AuNPs are reported. Singlet oxygen quantum yield, which is the main requirement for PDT, is reported in this work for the first time for any Pc–AuNP conjugate.

<sup>a</sup>Department of Chemistry, Rhodes University, Grahamstown 6140, South Africa.  
E-mail: [t.nyokong@ru.ac.za](mailto:t.nyokong@ru.ac.za)

<sup>b</sup>Gebze Institute of Technology, Department of Chemistry, Gebze 41400, Turkey



**Scheme 1** Synthesis route to phthalocyanine **7** (ZnPcSH). i: Tetraethylene glycol,  $K_2CO_3$ , DMF; ii: 2-Mercaptopyridine,  $K_2CO_3$ , DMF; iii:  $Zn(OAc)_2$ , pentanol, DBU; iv: Methane sulfonyl chloride, triethylamine, dichloromethane; v: (1) Thiourea, ethanol, THF, (2) NaOH, (3)  $H^+$ .

## Experimental

### Materials

Trisodium citrate (99%), gold(III) chloride trihydrate, sodium borohydride, tetraoctylammonium bromide (TAOBr), zinc phthalocyanine (ZnPc) and 1,3-diphenylisobenzofuran (DPBF) were purchased from Aldrich. 1,8-Diazabicyclo[5,4,0]undec-7-ene (DBU) was obtained from Fluka. Triethylamine, methane sulfonyl chloride and thiourea were obtained from Sigma-Aldrich.

4-Nitrothalonitrile (**1**)<sup>25</sup> 3-nitrothalonitrile (**2**),<sup>26</sup> 4-(2-(2-(2-(2-hydroxyethoxy)ethoxy)ethoxy)ethoxy)phthalonitrile (**3**)<sup>27–29</sup> and 3-(2-mercaptopyridine) phthalonitrile (**4**)<sup>30</sup> were synthesized and purified according to literature procedures. All solvents were dried and purified as described by Perrin and Armarego<sup>31</sup> before use. All other reagents were obtained from commercial suppliers and used without further purification.

### Equipment

The infrared (IR) spectra were recorded between 4000 and 650  $cm^{-1}$  using a Perkin Elmer Spectrum 100 FT-IR

spectrometer with an attenuated total reflection (ATR) accessory featuring a zinc selenide (ZnSe) crystal. The mass spectra were recorded on an LCQ-ion trap (Thermo Finnigan, San Jose, CA, USA), equipped with an ES (Electrospray) source and an MALDI (matrix assisted laser desorption ionization) BRUKER Microflex LT using 2,5-dihydroxybenzoic acid as a matrix.  $^1H$  NMR spectra were recorded in DMSO- $d_6$  solutions on a Varian 500 MHz spectrometer.

Ground state electronic absorption spectra were performed on a Shimadzu UV-2550 spectrophotometer. Fluorescence excitation and emission spectra were recorded on a Varian Eclipse spectrofluorimeter. Fluorescence lifetimes were measured using a time correlated single photon counting (TCSPC) setup (FluoTime 200, Picoquant GmbH). The excitation source was a diode laser (LDH-P-670 driven by PDL 800-B, 670 nm, 20 MHz repetition rate, 44 ps pulse width, Picoquant GmbH). Fluorescence was detected under the magic angle with a peltier cooled photomultiplier tube (PMT) (PMA-C 192-N-M, Picoquant) and integrated electronics (PicoHarp 300E, Picoquant GmbH). A monochromator with a spectral width of about 8 nm was used to select the required emission wavelength

band. The response function of the system, which was measured with a scattering Ludox solution (DuPont), had a full width at half-maximum (FWHM) of about 300 ps. The ratio of stop to start pulses was kept low (below 0.05) to ensure good statistics. All luminescence decay curves were measured at the maximum of the emission peak. The data were analysed with the program FluoFit (Picoquant).

The triplet decay kinetics data were collected on a laser flash photolysis system. The light pulses used in excitation were produced by a Quanta-Ray Nd:YAG laser (1.5 J/9 ns), pumping a Lambda Physik FL 3002 dye laser (Pyridin 1 in methanol). The analyzing beam source was from a Thermo Oriol 66902 xenon arc lamp, and a photomultiplier tube was used as a detector. Signals were recorded with a two channel, 300 MHz digital real time oscilloscope (Tektronix TDS 3032 C). The samples were placed in a 1 cm path length fluorescence spectrophotometric cell, degassed by bubbling argon for 30 min and irradiated at the Q band maxima. The triplet lifetimes were determined by exponential fitting of the kinetic curves using the Origin Pro 8 software.

Transmission electron microscope (TEM) images were obtained using a JEOL TEM 1210 transmission electron microscope at 100 kV accelerating voltage. TEM samples were prepared by placing a drop of conjugates or nanoparticle solution on the sample grid and allowing it to dry before measurements. X-ray powder diffraction patterns were recorded on a Bruker D8 Discover equipped with a LynxEye detector, using CuK $\alpha$  radiation ( $\lambda = 1.5405 \text{ \AA}$ , nickel filter). Data were collected in the range from  $2\theta = 5^\circ$  to  $100^\circ$ , scanning at  $1^\circ \text{ min}^{-1}$  with a filter time-constant of 2.5 s per step and a slit width of 6.0 mm. Samples were placed on a zero background silicon wafer slide. The X-ray diffraction data were treated using Eva (evaluation curve fitting) software. Baseline correction was performed on each diffraction pattern.

## Synthesis

**1,8(11),15(18)-Tri-(2-mercaptopyridine)-23(24)-4-(2-[2-[2-(2-hydroxyethoxy)-ethoxy]ethoxy]ethoxy) phthalocyaninato zinc(II) (5).** 4-(2-[2-[2-(2-Hydroxyethoxy)ethoxy]ethoxy]-ethoxy)phthalonitrile (3) (100 mg, 0.31 mmol), 3-(2-mercaptopyridine) phthalonitrile (4) (222.2 mg, 0.94 mmol), DBU (0.1 mL, 0.63 mmol) and Zn(OAc) $_2$  (114.4 mg, 0.63 mmol) were refluxed in dry pentanol (3 mL) for 24 h under an argon atmosphere. Then, the reaction mixture was cooled to room temperature and poured into *n*-hexane. The green solid product was precipitated and collected by filtration. The crude product (5) was purified over a silica gel column using firstly 25 : 1 and then a 10 : 1 dichloromethane : ethanol solvent mixture as an eluent. Yield: 50 mg (15%). IR [(ATR)  $\nu_{\text{max}}/\text{cm}^{-1}$ ]: 3400 (O-H), 3053 (Ar C-H), 2921–2864 (C-H), 1607 (C=N), 1571 (C=C), 1482, 1448, 1418, 1386, 1331, 1315, 1240, 1095 (C-O-C), 962, 896, 731. UV-Vis (DMSO):  $\lambda_{\text{max}}$  nm (log  $\epsilon$ ) 693 (4.81), 624 (4.14), 346 (4.43).  $^1\text{H}$  NMR (500 MHz, DMSO- $d_6$ ):  $\delta$ , ppm = 8.72–7.01 (m, 24H, Pc-H and Pyridyl-H), 4.22–3.12 (m, 16H, CH $_2$ ), 7.00 (s, 1H, O-H). Calc. for C $_{55}$ H $_{41}$ N $_{11}$ O $_5$ S $_3$ Zn: C 60.19; H 3.77; N

14.04; Found: C 60.42; H 3.81; N 14.20. MS (MALDI-TOF),  $m/z$  (%): Calc. 1097.59, Found 1098.42 [M + H] $^+$  (100).

**1,8(11),15(18)-Tri-(2-mercaptopyridine)-23(24)-4-(2-[2-[2-(2-methanesulfonyloxyethoxy)-ethoxy]ethoxy]ethoxy) phthalocyaninato zinc(II) (6).** Compound 5 (30 mg, 0.027 mmol) was dissolved in dichloromethane (10 mL) in the presence of triethylamine (20 drops, excess) and cooled down to  $\sim 0^\circ \text{C}$  in an ice bath. Methane sulfonyl chloride (10 drops, excess) was added drop-wise to the solution. The mixture was allowed to warm to room temperature and stirred for 30 min. The reaction was followed by thin-layer chromatography (TLC) using a 25 : 1 dichloromethane : ethanol solvent mixture as an eluent. When the starting compound 5 was completely consumed, the resulting solution was extracted with water and dichloromethane phase was dried with anhydrous sodium sulphate. Dichloromethane was removed and the crude product (6) was purified by preparative TLC (silica gel) using a 25 : 1 dichloromethane : ethanol solvent system as an eluent. Yield: 30 mg (94%). IR [(ATR)  $\nu_{\text{max}}/\text{cm}^{-1}$ ]: 3061 (Ar C-H), 2919–2851 (C-H), 1608 (C=N), 1571 (C=C), 1449, 1417, 1386, 1329, 1238, 1172 (S=O), 1096 (C-O-C), 963, 896, 804, 758, 740. UV-Vis (DMSO):  $\lambda_{\text{max}}$  nm (log  $\epsilon$ ) 693 (5.14), 630 (4.61), 343 (4.82).  $^1\text{H}$  NMR (500 MHz, DMSO- $d_6$ ):  $\delta$ , ppm = 8.89–6.99 (m, 24H, Pc-H and Pyridyl-H), 4.55–3.37 (m, 16H, CH $_2$ ), 3.15 (s, 3H, CH $_3$ ). Calc. for C $_{56}$ H $_{43}$ N $_{11}$ O $_7$ S $_4$ Zn: C 57.21; H 3.69; N 13.11; Found: C 57.54; H 3.88; N 13.45. MS (MALDI-TOF),  $m/z$  (%): Calc. 1175.68, Found 1176.97 [M + H] $^+$  (100).

**1,8(11),15(18)-Tri-(2-mercaptopyridine)-23(24)-4-(2-[2-[2-(2-mercaptoethoxy)-ethoxy]ethoxy]ethoxy) phthalocyaninato zinc(II) (7) (ZnPcSH).** A tetrahydrofuran (THF) (10 mL) and ethanol (3 mL) mixture was deoxygenated by sonication for 30 min using an ultrasonic bath. Compound 6 (20 mg, 0.018 mmol) was dissolved in this previously prepared solvent mixture and the solution was refluxed under an argon atmosphere in the dark. Then, thiourea (10 mg, excess) was added during reflux and the reaction was followed using TLC. After the starting compound 6 was consumed, argon was bubbled through the reaction mixture. Aqueous sodium hydroxide solution (20%, 4 mL) which was previously deoxygenated by sonication for 30 min was added and the mixture was refluxed for 2 h. When the reaction was complete (monitoring with TLC), the resulting mixture was poured into a mixture of dilute hydrochloric acid and ice and extracted with dichloromethane. The organic phase was extracted and dried with anhydrous sodium sulphate. The crude product (7, ZnPcSH) was purified by preparative TLC (silica gel) using a 10 : 1 dichloromethane : ethanol solvent system as an eluent. Yield: 12 mg (63%). IR [(ATR)  $\nu_{\text{max}}/\text{cm}^{-1}$ ]: 3079 (Ar C-H), 2919–2867 (C-H), 1603 (C=N), 1524 (C=C), 1481, 1449, 1386, 1323, 1279, 1238, 1109, 1081, 944, 895, 762, 741. UV-Vis (DMSO):  $\lambda_{\text{max}}$  nm (log  $\epsilon$ ) 693 (4.53), 643 (4.16), 343 (4.27).  $^1\text{H}$  NMR (500 MHz, DMSO- $d_6$ ):  $\delta$ , ppm = 9.48–7.48 (m, 24H, Pc-H and Pyridyl-H), 4.65–3.28 (m, 16H, CH $_2$ ), 7.09 (s, 1H, S-H). Calc. for C $_{55}$ H $_{41}$ N $_{11}$ O $_4$ S $_4$ Zn: C 59.32; H 3.71; N 13.83; Found: C 59.61; H 3.94; N 13.78. MS (ES-MS),  $m/z$  (%): Calc. 1113.66, Found 1136.17 [M + Na] $^+$  (100).

### Conjugation of ZnPcSH to gold nanoparticles

Synthesis of TAOBr stabilized AuNPs has been reported before.<sup>32–34</sup> ZnPcSH was conjugated using the method employed by Kotiaho *et al.* with modifications.<sup>32</sup> The toluene solution of gold nanoparticles was evaporated to about 1.5 mL and 1.5 mg (0.0013 mmol) of ZnPcSH was added. The solution was stirred for 24 h to allow ligand exchange. The Pc–AuNPs conjugate was purified using Bio-Beads and toluene as an eluent.

### Photophysical and photochemical parameters

Fluorescence quantum yields ( $\Phi_F$ ) were determined by a comparative method<sup>35</sup> using eqn (1):

$$\Phi_F = \Phi_{F(\text{std})} = \frac{FA_{\text{std}}n^2}{F_{\text{std}}An_{\text{std}}^2} \quad (1)$$

where  $F$  and  $F_{\text{std}}$  are areas under fluorescence emission curves of the samples (ZnPcSH or ZnPcSH–AuNPs) and the standard respectively.  $A$  and  $A_{\text{std}}$  are the absorbances of the samples and the standard at the excitation wavelength and  $n$  and  $n_{\text{std}}$  are refractive indices of solvents used for the samples and the standard, respectively. ZnPc in DMSO was used as a standard,  $\Phi_F = 0.20$  for the determination of fluorescence quantum yields.<sup>36</sup> The sample and the standard were both excited at the same relevant wavelength.

The triplet quantum yields were determined by eqn (2).

$$\Phi_T = \Phi_T^{\text{Std}} \frac{\Delta A_T \varepsilon_T^{\text{Std}}}{\Delta A_T^{\text{Std}} \varepsilon_T} \quad (2)$$

where  $\Delta A_T$  and  $\Delta A_T^{\text{Std}}$  are the changes in the triplet state absorbances of the samples and the standard respectively.  $\varepsilon_T$  and  $\varepsilon_T^{\text{Std}}$  are the triplet state molar extinction coefficients for the samples and the standard respectively.  $\Phi_T^{\text{Std}}$  is the triplet state quantum yield for the unsubstituted ZnPc standard ( $\Phi_T^{\text{Std}} = 0.65$  for ZnPc in DMSO).<sup>37</sup>

$\varepsilon_T$  and  $\varepsilon_T^{\text{Std}}$  were calculated from the molar extinction coefficients of their respective ground singlet state ( $\varepsilon_S$  and  $\varepsilon_S^{\text{Std}}$ ), the change in absorbances of the ground states ( $\Delta A_S$  and  $\Delta A_S^{\text{Std}}$ ) and the change in the triplet state absorptions ( $\Delta A_T$  and  $\Delta A_T^{\text{Std}}$ ) using eqn (3a) and (3b).

$$\varepsilon_T = \varepsilon_S \frac{\Delta A_T}{\Delta A_S} \quad (3a)$$

$$\varepsilon_T^{\text{Std}} = \varepsilon_S^{\text{Std}} \frac{\Delta A_T^{\text{Std}}}{\Delta A_S^{\text{Std}}} \quad (3b)$$

### Singlet oxygen quantum yield

Singlet oxygen quantum yield ( $\Phi_\Delta$ ) values were determined in air using the relative method with DPBF as a singlet oxygen quencher in DMSO. Eqn (4) was used for calculating singlet oxygen quantum yields:

$$\Phi_\Delta = \Phi_\Delta^{\text{Std}} \frac{R^{\text{Sample}} I^{\text{Std}}}{R^{\text{Std}} I^{\text{Sample}}} \quad (4)$$

where ( $\Phi_\Delta^{\text{Std}}$ ) is the singlet oxygen quantum yield for the standard (ZnPc,  $\Phi_\Delta^{\text{Std}} = 0.67$  in DMSO).<sup>38</sup>  $R^{\text{Sample}}$  and  $R^{\text{Std}}$  are the DPBF photobleaching rates in the presence of the respective sample under investigation and the standard respectively.  $I^{\text{Sample}}$  and  $I^{\text{Std}}$  are the rates of light absorption by the sample and the standard respectively.

Solutions of the complexes (ZnPcSH and ZnPcSH–AuNPs) with an absorbance of  $\sim 0.3$  at the irradiation wavelength were prepared in the dark and irradiated at the Q-band. DPBF absorption at 417 nm was monitored with photolysis time.

## Results and discussion

### Synthesis and characterization

**ZnPcSH complex.** The synthesis of phthalonitrile derivatives (1 to 4, Scheme 1) was previously reported.<sup>25–30</sup> The synthesis of unsymmetrical phthalocyanines is complicated compared to symmetrically substituted Pcs as they often require extensive purification methods to obtain the desired products. Scheme 1 shows the chemical structure and the synthetic route of compound 7. The statistical condensation method of two phthalonitriles 3 and 4 was employed in this work. The synthesis of complex 7 starts with the synthesis of 5. The reaction for the formation of 5 was performed by a statistical method using a 3:1 ratio of phthalonitrile 3 (A):phthalonitrile 4 (B). As a result, isomers were obtained in different amounts during the synthesis of compound 5. We focused on the AB3 type isomer (compound 5) in this study and this Pc derivative was separated by using column chromatography from the isomeric mixture. We also aimed at the synthesis of compound 7 which contains only one SH group from compound 5 for attachment of this compound to Au nanoparticles *via* an SH group.

The terminal hydroxyl group on complex 5 was converted into its mesylate counterparts using triethylamine (TEA) followed by the addition of methanesulfonyl chloride to give the substituted phthalocyanine 6. Finally, the terminal thiol functional group was obtained under an inert atmosphere in the absence of light, in a previously degassed THF–ethanol solvent mixture containing complex 6. The resultant product was then hydrolysed using 20% NaOH (also previously degassed). The inert atmosphere inhibits the formation of disulfides *via* aerobic oxidations and ensures the formation of complex 7.

Characterization of complexes of 5–7 was achieved using infra-red (IR), ultraviolet-visible (UV-Vis), matrix-assisted laser desorption/ionization-time of flight (MALDI-TOF) and proton nuclear magnetic resonance (<sup>1</sup>H NMR) spectroscopies as well as elemental analyses. The <sup>1</sup>H NMR spectrum of the target complex 7 showed aromatic protons between 7.48 and 9.48 (integrating for 24 protons), the CH<sub>2</sub> groups between 3.28 and 4.65 (integrating for 16 protons) and the SH group at 7.09 (integrating for 1 SH proton). The mass spectrum of the complex showed a molecular ion peak at 1136.17 amu as an M + Na peak.

The UV-Vis spectrum of ZnPcSH is shown in Fig. 1A. It shows broadening typical of aggregation with a broad peak

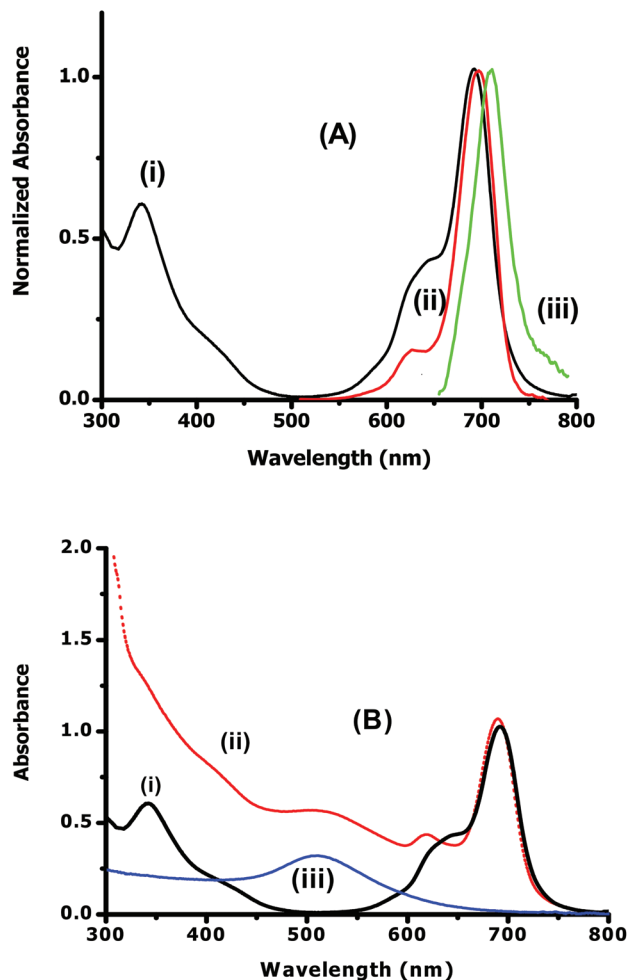


**Fig. 1** (A) (i) Absorption, (ii) excitation and (iii) emission spectra of ZnPcSH and (B) absorption spectra of (i) ZnPcSH, (ii) ZnPcSH-AuNPs and (iii) AuNPs complex in DMSO.

near 630 nm<sup>39</sup> and a more intense and sharper peak at 694 nm due to the monomer. However ZnPcSH obeys Beer's law at concentrations lower than  $2 \times 10^{-6}$  M in DMSO. The spectrum of ZnPcSH is red shifted (at 694 nm) compared to unsubstituted ZnPc (at 672 nm in DMSO), due to the presence of sulphur groups and non-peripheral substitution.

The absorption, excitation and emission of the ZnPcSH complex are shown in Fig. 1 (and Table 1). A slight red shift of the excitation compared to absorption spectra could be a result of different types of equipment used. The excitation spectrum is narrower than the absorption spectrum due to aggregation in the latter. Aggregates do not fluoresce. The excitation spectrum is the mirror image of the emission spectrum.

### AuNPs and ZnPcSH-AuNP conjugates

Phthalocyanine-functionalised gold nanoparticles were synthesized using a ligand exchange process, where the loosely bound TOABr ligands were partially exchanged by Pcs that bind covalently to the nanoparticle surface. The ZnPcSH complex is most likely attached to the AuNPs surface *via* an

**Table 1** Spectral, photophysical and photochemical parameters of ZnPcSH and ZnPcSH-AuNPs in DMSO

Parameter <sup>a</sup>	ZnPcSH	ZnPcSH-AuNP
$\lambda_{\text{abs}}$	694	692
$\lambda_{\text{exc}}$	695	694
$\lambda_{\text{emm}}$	708	706
$\Phi_{\text{F}}$	0.06	0.04
$\tau_{\text{F}}$ (ns) <sup>b</sup>	$3.08 \pm 0.02$	$2.38 (0.65) \pm 0.02$ $1.54 (0.35) \pm 0.01$
$\tau_0$ (ns)	51.33	$78.75^c$
$\Phi_{\text{T}}$	0.63	0.84
$\tau_{\text{T}}$ ( $\mu\text{s}$ )	217	455
$\Phi_{\Delta}$	0.45	0.68

<sup>a</sup>  $\lambda_{\text{abs}}$  = absorption wavelength,  $\lambda_{\text{exc}}$  = excitation wavelength,  $\lambda_{\text{emm}}$  = emission wavelength. <sup>b</sup> Amplitudes in brackets. <sup>c</sup> Average lifetime used.

Au-S bond due to the SH group terminating the ethoxy ligand. However, it is possible that the sulphur atoms of the mercapto group also coordinate to the AuNPs. It is expected that the stronger bond will be that of the SH group, resulting in a mainly perpendicular arrangement on the AuNPs.

The surface plasmon resonance (SPR) peak was observed at around 510 nm for both gold nanoparticles (AuNPs) and ZnPcSH-AuNPs conjugate (Fig. 1B). A blue shift of about 2 nm was observed in the absorption spectrum of the ZnPcSH-AuNPs conjugate from that of the ZnPcSH. A blue shift usually implies that the sulphur groups (which result in red shifting in phthalocyanines) are engaged with AuNPs. However, the blue shift in Fig. 1B is very small. Such small blue shifts have been observed on conjugation of Pcs to AuNPs.<sup>11</sup> The spectrum of ZnPcSH in the presence of AuNPs is broad due to the absorption of the latter.

Fig. 2 shows the absorption, excitation and emission spectra of the ZnPcSH-AuNPs conjugate. The absorption is broadened due to the SPR band of AuNPs. This band is not observed on the excitation or emission spectra since AuNPs do not fluoresce. The excitation spectrum is the mirror image of the emission spectrum for ZnPcSH-AuNPs as was the case for ZnPcSH alone.

The average size of the AuNPs and its conjugate was determined by powdered XRD of AuNPs and ZnPcSH-AuNPs using the Scherrer eqn (5):<sup>40</sup>

$$d(\text{\AA}) = \frac{k\lambda}{\beta \cos\theta} \quad (5)$$

where  $k$  is an empirical constant equal to 0.9,  $\lambda$  is the wavelength of the X-ray source (1.5405  $\text{\AA}$ ),  $\beta$  is the full width at half maximum of the diffraction peak, and  $\theta$  is the angular position of the peak. The XRD patterns of TOABr-AuNPs and ZnPcSH-AuNPs were both indexed to a face centred cubic structure of gold nanoparticles (Fig. 3). The sharper peaks observed for AuNPs suggest crystallinity which becomes less on conjugation of the AuNPs to ZnPcSH, Fig. 3B. The estimated average size of the TOABr-AuNPs and Pc-AuNPs was 5.3 nm and 17 nm, respectively, using the peak at  $37.58^\circ$  (corresponding to gold). The large size of ZnPcSH-AuNPs suggests aggregation.

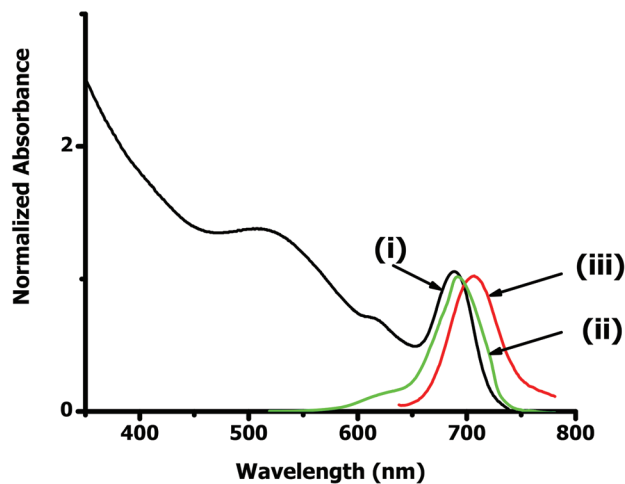


Fig. 2 (i) Absorption, (ii) excitation and (iii) emission spectra of a ZnPcSH-AuNPs complex in DMSO.

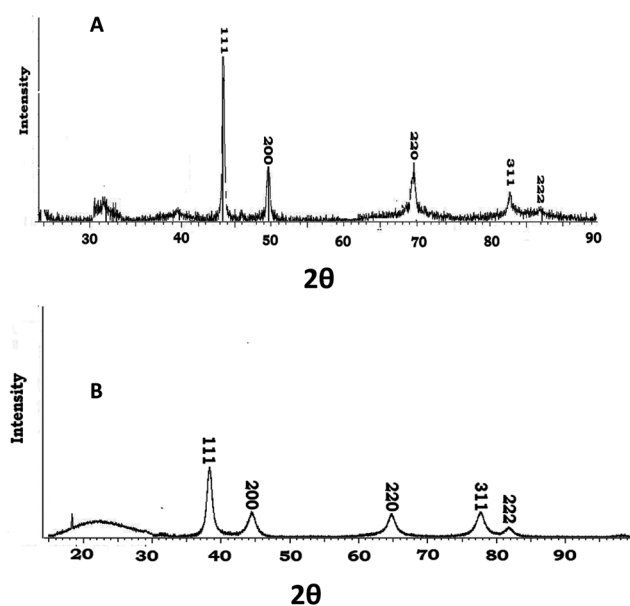


Fig. 3 XRD patterns of (A) TAOBr-AuNPs and (B) ZnPcSH-AuNPs.

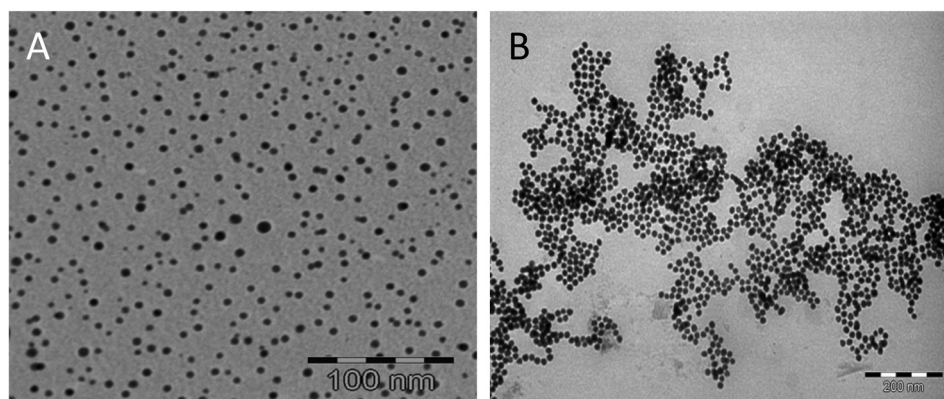


Fig. 4 TEM micrographs of (A) TAOBr-AuNPs and (B) ZnPcSH-AuNPs.

TEM micrographs of the AuNPs and ZnPcSH-AuNPs are shown in Fig. 4. Fig. 4A shows monodispersed spherical AuNPs with an average particle size of 5.5 nm, which is similar to the one determined using XRD. Upon conjugation with a ZnPcSH complex the particles show slight aggregation (Fig. 4B), with an estimated average size of 16.2 nm corresponding to the values from XRD.

#### Fluorescence quantum yields and lifetimes

Fluorescence quantum yields and lifetimes are important characteristics of a photosensitizer since molecules with high fluorescence quantum yields usually have correspondingly low triplet quantum yields. A slight decrease in the fluorescence quantum yield was observed for ZnPcSH after conjugation with AuNPs (Table 1). The fluorescence quantum yield for ZnPcSH is lower than typical of Pc complexes<sup>3</sup> and much lower than that of the ZnPc standard.<sup>36</sup> The decrease in fluorescence in the presence of heavy metals is often associated with the population of the triplet state of the molecule.<sup>41</sup> This decrease of the fluorescence quantum yield has been observed previously for gold nanoparticles-fluorophore systems,<sup>7,33,34,42</sup> due to the heavy atom effect of the AuNPs. The fluorescence lifetimes of both complexes as determined by the photon counting method are also reported in Table 1 and the decay curve is shown in Fig. 5. The measured lifetime of the ZnPcSH complex was 3.08 ns whereas a ZnPcSH-AuNPs conjugate showed two lifetimes of 2.38 and 1.54 ns. A plausible explanation for two lifetimes is that there may be two different conjugation systems due to different orientation and packing of Pc molecules on the AuNP surfaces. This is due to reports that when single peripheral tethers were used (as is the case in this work), the macrocycle rings were found to be tilted at various angles to the substrate surface,<sup>8</sup> with flat orientation being achieved in some cases, but often, various degrees of tilt are obtained. This is opposed to when octasubstituted rings are employed where the so called “octopus” orientation is observed.<sup>8</sup>

The quenching of lifetimes may be explained using fluorescence radiative lifetime ( $\tau_0$ ), which measures the lifetime of

the molecule in the absence of the non-radiative processes. This lifetime is directly connected to absorption coefficients and excited state lifetimes and hence can be calculated from the measurement of fluorescence quantum yield ( $\Phi_F$ ) and lifetime ( $\tau_F$ ) using eqn (6).<sup>43</sup>

$$\tau_0 = \tau_F / \Phi_F \quad (6)$$

The  $\tau_0$  values were higher than the measured fluorescence lifetimes ( $\tau_F$ ) (Table 1). The large values of  $\tau_0$  compared to  $\tau_F$  are not surprising because non-radiative processes cause faster fluorescence decay. The larger values of  $\tau_0$  have also been reported previously for various phthalocyanines and in similar studies.<sup>44,45</sup> A ZnPcSH–AuNPs conjugate was found to have a higher  $\tau_0$  as compared to a ZnPcSH complex. The radiative lifetime ( $\tau_0$ ) in the presence of metal particles can either increase or decrease depending on the molecular dipole and the distance between the fluorophore and the metal. According to the studies done previously by Lakowicz,<sup>46,47</sup> the radiative rate will increase when the oscillating dipole is not in line with the

reflected field.<sup>46,47</sup> Therefore the observed increase in  $\tau_0$  when the phthalocyanine was attached to the gold surface could suggest an uncorrelated field.

### Triplet quantum yields and lifetimes

Triplet quantum yields and lifetimes determine the ability of the photosensitizer to produce singlet oxygen. Triplet quantum yield values are shown in Table 1 (decay curves shown in Fig. 6). Upon conjugation with AuNPs the triplet quantum yield increased from 0.63 to 0.84. This effect shows that the presence of gold nanoparticles enhances the triplet state population. This enhancement of triplet quantum yield could also be the contribution of the bromide ion present in the nanoparticles from the tetraoctylammonium bromide used in the synthesis.<sup>9</sup> The triplet lifetime of a ZnPcSH–AuNPs conjugate (455  $\mu$ s) was larger than that of the ZnPcSH complex alone (217  $\mu$ s). This further shows that the triplet state was favoured in the presence of the AuNPs. The observation of increased triplet quantum yield and lifetimes in the presence of nanoparticles is not in agreement with what is expected, where increase in triplet yields is expected to be accompanied by a decrease in lifetime. The increase in the triplet lifetimes in the presence of Au nanoparticles has been regularly observed<sup>33</sup> and it could be a result of the protection of the Pc from the environment by the former.

### Singlet oxygen quantum yields

Singlet oxygen is produced when photosensitizers in the excited triplet state transfer energy to the molecular oxygen. Thus singlet oxygen quantum yield ( $\Phi_\Delta$ ) is the measure of the efficiency of singlet oxygen production. The photo-degradation of the singlet oxygen quencher (DPBF) suggests the ability of the complexes (ZnPcSH and ZnPcSH–AuNPs) to produce singlet oxygen. Fig. 7 (A and B) shows time dependent degradation of DPBF upon irradiation. A higher singlet oxygen quantum yield of 0.68 was observed for ZnPcSH–AuNPs as compared to 0.45 of ZnPcSH. The

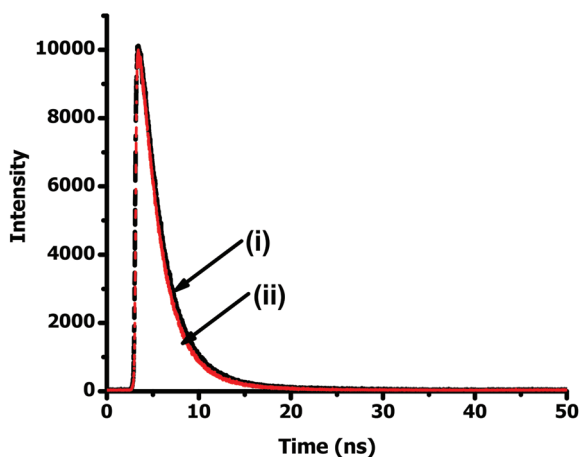


Fig. 5 Fluorescence decay curves of (i) ZnPcSH and (ii) ZnPcSH–AuNPs in DMSO.

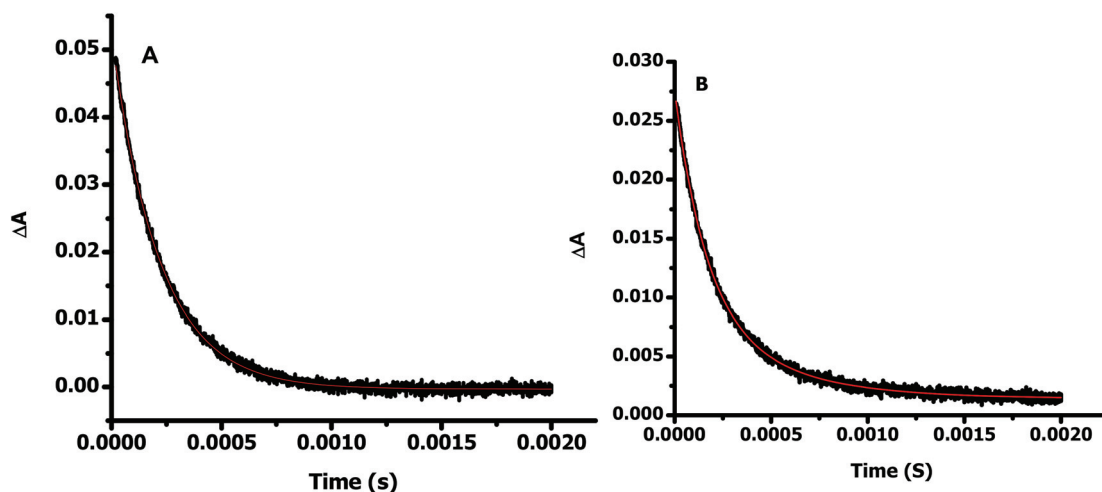


Fig. 6 Triplet decay curves of (A) ZnPcSH and (B) ZnPcSH–AuNPs in DMSO.

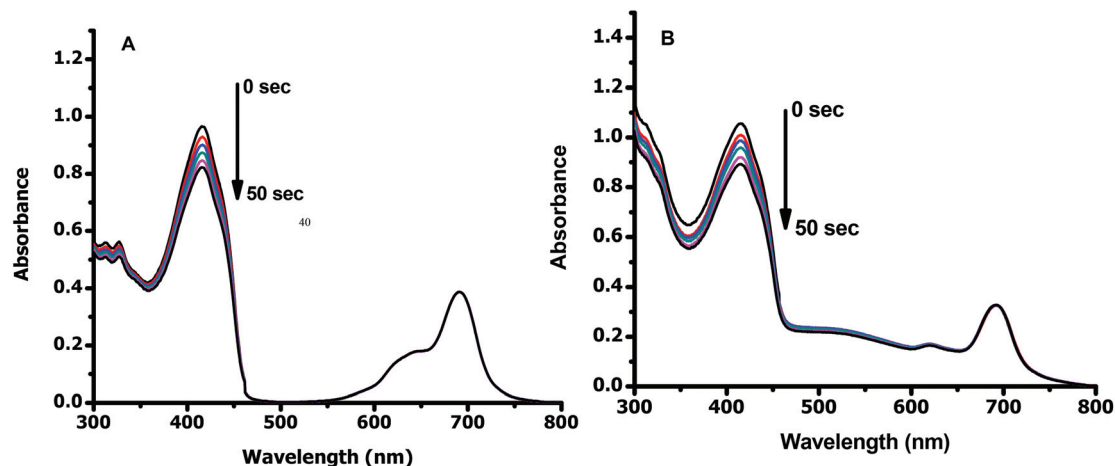


Fig. 7 Photodegradation of DPBF in the presence of (A) ZnPcSH and (B) ZnPcSH-AuNPs in DMSO.

Q-band of the phthalocyanine remained unchanged in both complexes.

## Conclusions

A novel zinc phthalocyanine complex which contains a free thiol group was successfully synthesized and characterized. The complex was successfully conjugated to gold nanoparticles *via* ligand exchange. The surface plasmon peak of gold nanoparticles was observed on the UV-Vis spectrum of the conjugate and a blue shift showed the formation of the conjugate. The fluorescence quantum yield and lifetime decreased on conjugation. There was an increase in the triple quantum yield and lifetime upon conjugation. The increase in the triplet quantum yield was followed by an increase in the singlet oxygen quantum yield upon conjugation.

## Acknowledgements

This work was supported by the Department of Science and Technology (DST)/Nanotechnology (NIC) and National Research Foundation (NRF) of South Africa through DST/NRF South African Research Chairs Initiative for Professor of Medicinal Chemistry and Nanotechnology and Rhodes University.

## References

- 1 T. J. Dougherty, C. J. Gomer, B. W. Henderson, G. Jori, D. Kessel, M. Korbelik, J. Moan and Q. Peng, *J. Natl. Cancer Inst.*, 1998, **90**, 889–905.
- 2 T. Nyokong, in *N4-Macrocyclic metal complexes: electrocatalysis, electrophotochemistry, and biomimetic electrocatalysis*, ed. J. H. Zagal, F. Bedioui and J.-P. Dodelet, Springer, 2006, ch. 7, ISBN0-387-28429.
- 3 T. Nyokong and E. Antunes, in *The Handbook of Porphyrin Science*, ed. K. M. Kadish, K. M. Smith and R. Guilard, Academic Press, New York, vol. 7, 2010, ch. 34, pp. 247–349, World Scientific, Singapore.
- 4 M. Hanack, T. Schneider, M. Bartheb, J. S. Shirk, S. R. Flom and R. G. S. Pong, *Coord. Chem. Rev.*, 2001, **219–221**, 235–258.
- 5 K. I. Ozoemena and T. Nyokong, *Inorg. Chem. Commun.*, 2003, **6**, 1192–1195.
- 6 M. C. G. Vior, L. E. Dicellio and J. Awruch, *Dyes Pigm.*, 2009, **83**, 375–380.
- 7 B. Ogunsipe, M. Durmuş, D. Atilla, A. G. Gürek, V. Ahsen and T. Nyokong, *Synth. Met.*, 2008, **158**, 839–847.
- 8 Z. Li and M. Lieberman, *Langmuir*, 2001, **17**, 4887–4894.
- 9 D. C. Hone, P. I. Walker, R. Evans-Gowing, S. FitzGerald, A. Beeby, I. Chambrier, M. J. Cook and D. A. Russell, *Langmuir*, 2002, **18**, 2985–2987.
- 10 M. Camerin, M. Magaraggia, M. Soncin, G. Jori, G. M. Moreno, I. Chambier, M. J. Cook and D. A. Russell, *Eur. J. Cancer*, 2010, **46**, 1910–1918.
- 11 N. Nombona, E. Antunes, C. Litwinski and T. Nyokong, *Dalton Trans.*, 2011, **40**, 11876–11884.
- 12 M. Göksel, M. Durmuş and D. Atilla, *J. Porphyrins Phthalocyanines*, 2012, **16**, 895–906.
- 13 E. Ruoslanti, S. N. Bhatia and M. J. Sailor, *J. Cell Biol.*, 2010, **188**, 759–768.
- 14 N. J. Nam, S. I. Steva and C. A. Mirkin, *J. Am. Chem. Soc.*, 2004, **126**, 5932–5933.
- 15 R. Wilson, *Chem. Soc. Rev.*, 2008, **37**, 2028–2045.
- 16 G. Han, P. Ghosh and V. M. Rotello, *Nanomedicine*, 2007, **2**, 113–123.
- 17 H. Hiramatsu and F. E. Osterloh, *Chem. Mater.*, 2004, **16**, 2509–2511.
- 18 H. Hussain, S. Graham, Z. Wang, B. Tan, D. C. Sherrington, S. P. Rannard, A. I. Cooper and M. Brust, *J. Am. Chem. Soc.*, 2005, **127**, 16398–16399.
- 19 Z. Wang, B. Tan, I. Hussain, N. Schaeffer, M. F. Wyatt, M. Brust and A. I. Cooper, *Langmuir*, 2007, **23**, 885–895.

- 20 S. D. Perrault and W. C. W. Chan, *J. Am. Chem. Soc.*, 2009, **131**, 17042–17043.
- 21 R. G. Shimmin, A. B. Schoch and P. V. Braun, *Langmuir*, 2004, **20**, 5613–5620.
- 22 H. Otsuka, Y. Nagasaki and K. Katoaka, *Adv. Drug Deliv. Rev.*, 2003, **55**, 403–419.
- 23 N. Wangoo, K. K. Bhasin, S. K. Mehta and C. R. Suri, *J. Colloid Interface Sci.*, 2008, **232**, 247–254.
- 24 Y. Liu, Y. Liu, R. L. Mernaugh and X. Zheng, *Biosens. Bioelectron.*, 2009, **24**, 2853–2857.
- 25 J. G. Young and W. Onyebuagu, *J. Org. Chem.*, 1990, **55**, 2155–2159.
- 26 R. D. George and A. W. Snow, *J. Heterocycl. Chem.*, 1995, **32**, 495–498.
- 27 M. Karabork and S. Serin, *Synth. React. Inorg., Met.-Org., Nano-Met. Chem.*, 2002, **32**, 1635–1647.
- 28 U. Kumru, M. A. Ermeydan, F. Dumoulin and V. Ahsen, *J. Porphyrins Phthalocyanines*, 2008, **12**, 1090–1095.
- 29 S. Tuncel, F. Dumoulin, J. Gailer, M. Sooriyaarachchi, D. Atilla, M. Durmuş, D. Bouchu, H. Savoie, R. W. Boyle and V. Ahsen, *Dalton Trans.*, 2011, **40**, 4067–4079.
- 30 N. Sehlotho, M. Durmuş, V. Ahsen and T. Nyokong, *Inorg. Chem. Commun.*, 2008, **11**, 479–483.
- 31 D. D. Perrin and W. L. F. Armarego, *Purification of Laboratory Chemicals*, Pergamon Press, Oxford, 2nd edn, 1989.
- 32 A. Kotiaho, R. Lahtinen, A. Efimov, H. Lehtivuori, N. V. Tkachenko, T. Kanerva and H. Lemmetyinen, *J. Photochem. Photobiol. A: Chem.*, 2010, **212**, 129–134.
- 33 N. Masilela and T. Nyokong, *J. Photochem. Photobiol. A: Chem.*, 2011, **223**, 124–131.
- 34 S. Tombe, W. Chidawanyika, E. Antunes, G. Priniotakis, P. Westbroek and T. Nyokong, *J. Photochem. Photobiol. A: Chem.*, 2012, **240**, 50–58.
- 35 S. Frey-Forgues and D. Lavabre, *J. Chem. Educ.*, 1999, **76**, 1260–1264.
- 36 A. Ogunsipe, J. Y. Chen and T. Nyokong, *New J. Chem.*, 2004, **28**, 822–827.
- 37 T. H. Tran-Thi, C. Desforge and C. C. Thiec, *J. Phys. Chem.*, 1989, **93**, 1226–1233.
- 38 N. Kuznetsova, E. A. Makarova, S. N. Dashkevich, N. S. Gretsova, E. A. Kalmykova, V. M. Negrimovsky, O. L. Kaliya and E. A. Lukyanets, *Russ. J. Gen. Chem.*, 2000, **70**, 140–148.
- 39 T. Nyokong and H. Isago, *J. Porphyrins Phthalocyanines*, 2004, **8**, 1083–1090.
- 40 S. Sapra, D. Sarma and D. Pramana, *J. Phys.*, 2005, **65**, 565–570.
- 41 E. A. Gastilovich, N. V. Korol'kova, V. G. Klimenko and R. N. Nurmukhametov, *Opt. Spectrosc.*, 2008, **104**, 491–494.
- 42 A. Kotiaho, R. Lahtinen, A. Efimov, H. Metsberg, E. Sariola, H. Lehtivuori, N. V. Tkachenko and H. Leetyinen, *J. Phys. Chem. C*, 2010, **114**, 162–168.
- 43 C. D. Geddes and J. R. Lakowicz, *Topics in Fluorescence Spectroscopy*, Springer, New York, 2005.
- 44 Y. Kaneko, Y. Nishimura, N. Takane, T. Arai, H. Sakuragi, N. Kobayashi, D. Matsunaga, C. Pac and K. Tokumaru, *J. Photochem. Photobiol. A*, 1997, **106**, 177–183.
- 45 T. P. Mthethwa, Y. Arslanoglu, E. Antunes and T. Nyokong, *Polyhedron*, 2012, **38**, 169–177.
- 46 J. R. Lakowicz, *Anal. Biochem.*, 2001, **298**, 1–24.
- 47 J. R. Lakowicz, *Anal. Biochem.*, 2005, **337**, 171–194.